

O.M. Popovych, I.M. Budzulyak, V.O. Kotsyubynsky, V.M. Boychuk, R.V. Ilnytskyi,  
M.M. Khemii, N.Ya. Ivanichok, Ye.V. Lezun

## **Ultrasonic Modification of Nanocrystalline NiMoO<sub>4</sub> Hydrate Obtained by Hydrothermal Method**

*Vasyl Stefanyk Precarpathian National University, Ivano-Frankivsk, Ukraine, [khemiolha@gmail.com](mailto:khemiolha@gmail.com)*

The paper presents the results of studies of the crystal structure, surface morphology and electrical properties of nickel molybdate obtained by hydrothermal method and modified by ultrasound. The influence of the duration of ultrasonic dispersion on the crystallites size, specific surface area, pore size distribution and activation energy of charge carriers of nickel molybdate hydrate is determined. It was found that ultrasound with a frequency of 22 kHz and a duration of 90 min leads to an increase in the total volume of mesopores from 0.135 cm<sup>3</sup>/g to 0.223 cm<sup>3</sup>/g with an average diameter of 28.5 nm.

**Keywords:** nickel molybdate hydrate, ultrasonic modification, specific surface area, conductivity.

*Received 23 February 2022; Accepted 2 June 2022.*

### **Introduction**

Electrochemical supercapacitors with high specific power, fast charge/discharge time and long cycle stability are one of the promising candidates for use in environmentally friendly energy storage devices. However, electrochemical supercapacitors have a lower specific energy compared to batteries [1]. Therefore, significant efforts of researchers are aimed at finding electroactive materials capable of storing energy through rapid redox reactions at the electrode/electrolyte interface and Faraday reactions associated with intercalation/deintercalation of ions into the material structure. In particular, transition metals oxides are widely studied as cathodes of hybrid capacitors, and anodes are carbon materials that accumulate charge by forming a double electric layer [2, 3]. Nickel and molybdenum oxides are excellent candidates for such applications due to their high redox activity, semiconductor properties and low cost [4]. However, to increase the capacitive characteristics of nickel molybdates, it is necessary to improve the transport kinetics of ions and electrons in the structure of the electrodes and at the electrode/electrolyte interface.

Ultrasonic dispersion is an effective method of modifying nanosized materials without the use of high temperatures, pressures and long reaction times [5, 6]. The speed of sound in the liquid varies from 1000 to 1500 m/s, and the lengths of ultrasonic waves are from 10 cm to 100 mm with frequencies from 20 kHz to 15 MHz [7]. These ultrasonic wavelengths are much larger than the size of molecules, so there is an obvious lack of direct interaction of the acoustic field with chemicals at the molecular level. In a liquid medium, ultrasonic irradiation of materials leads to two effects: chemical, which consists in the generation of radicals, and physical, which results in turbulence, mass transfer, micro flow, shock waves, etc. The chemical effects of ultrasonic irradiation are the result of acoustic cavitation, namely the formation, growth and implosive destruction of bubbles in a liquid medium, which instantly leads to a high temperature of ~ 5000 K and a pressure of ~ 1000 atm [7]. Bubbles are generated from pre-existing impurities and oscillate with the applied sound field. The stage leading to the growth of the bubble occurs due to the diffusion of solute vapor into the volume of the bubble. Oscillatory bubbles can efficiently store ultrasonic energy as they grow to a certain size (usually tens of μm). The last stage - the collapse of the bubble, occurs when its radius reaches its maximum value with the

release of energy in a very short time (with heating and cooling rate  $> 10^{10}$  K/s) [8]. At a frequency of 20 kHz, the critical diameter of the cavity is 170  $\mu\text{m}$ .

Thus, acoustic cavitation is a promising way to control the change in particle size and surface area of nanomaterials. For effective ultrasonic modification of the studied materials and minimization of energy losses, it is necessary to determine the optimal duration of ultrasonic exposure, at which the cavitation process will be the most effective. Therefore, we analyzed the crystal structure, surface morphology and conductive properties of nickel molybdate obtained by hydrothermal method and subjected to different times of ultrasonic dispersion.

## I. Materials and methods

$\text{NiMoO}_4$  hydrate was obtained by hydrothermal method, the synthesis procedure is described in the previous article [9]. Ultrasonic modification of the material was carried out for 15, 60 and 90 min in distilled water using an ultrasonic dispersant, the operating frequency of which is 22 kHz. The ultrasonic dispersant works on the principle of cavitation generation, in which high-power ultrasound is introduced into the liquid medium, causing sound waves to be transmitted in the liquid and create periodic cycles of high pressure (compression) and low pressure (rarefaction). The initial nickel molybdate hydrate was designated as  $\text{NiMoO}_4$ , a nickel molybdate hydrate that was sonicated for 15 min as  $\text{NiMoO}_4$ -15, for 60 min as  $\text{NiMoO}_4$ -60 and for 90 min as  $\text{NiMoO}_4$ -90.

The crystal structure was investigated by powder X-ray diffraction analysis using a diffractometer DRON (Cu-K $\alpha$  radiation, wavelength 0.15405 nm). The morphological properties were investigated by the low-temperature nitrogen absorption / desorption porosimetry (Quantachrome Autosorb Nova 2200e device). Electrical conductivity was studied using the AUTOLAB PGSTAT12 measuring complex in the frequency range  $10^{-2}$ -  $10^5$  Hz at a voltage of 0 V, in the temperature range 25 - 200  $^{\circ}\text{C}$ . The samples were pressed into a cylindrical mold with a diameter of 14 mm and a material thickness of 1 mm.

## II. Results and discussions

The X-ray diffraction patterns of the initial hydrothermally obtained nickel molybdate and ultrasonically modified materials are presented in Fig. 1. Diffraction peaks agree well with previously published data for nickel molybdate hydrate [10, 11]. In particular, the diffraction peaks at 27.1, 29.6, 33.2 and 36.4 $^{\circ}$  are consistent with the standard template for  $\text{NiMoO}_4 \cdot \text{H}_2\text{O}$  (JCPDS Card No. 13-0128), but the refinement of the crystal structure parameters is difficult. In the Raman spectra of  $\text{NiMoO}_4$  hydrate [9] we did not find any vibrational modes responsible for nitrates, nickel hydroxide or molybdenum oxide, which indicates the formation of single-phase nickel molybdate hydrate in hydrothermal synthesis. The synthesis resulted in  $\text{NiMoO}_4$

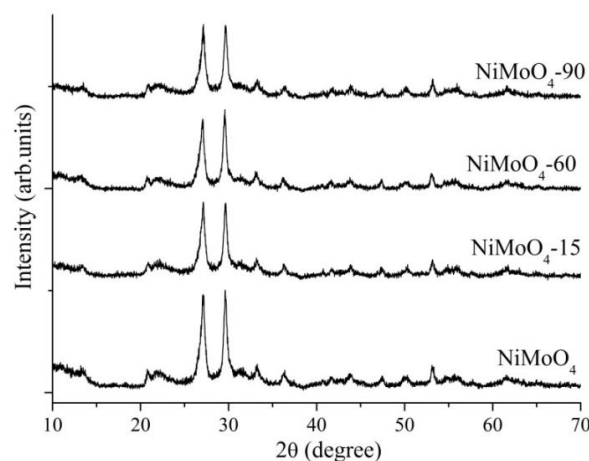


**Fig. 1.** X-ray diffraction patterns of the initial  $\text{NiMoO}_4$  hydrate obtained by hydrothermal method and modified by ultrasound for 15, 60 and 90 min.

hydrate with a triclinic crystal structure corresponding to the  $P\bar{1}$  space group. The crystal structure of  $\text{NiMoO}_4$  hydrate is composed of pairs of  $\text{NiO}_6$  and  $\text{NiO}_5(\text{H}_2\text{O})$  octahedra (water molecules coordinated with nickel atoms) connected by  $\text{MoO}_4$  tetrahedra, as well as lattice water not bound to other atoms and released when the hydrate is heated to 400  $^{\circ}\text{C}$ . The average size of the crystallites, calculated by the Scherrer equation:  $D = 0.9\lambda/\beta\cos\theta$ , where  $\lambda = 0.15405$  nm is the wavelength of Cu-K $\alpha$  radiation,  $\beta$  is the full width at half maximum,  $\theta$  is the angle corresponding to the maximum intensity peaks on the diffraction pattern, is 17 nm for all samples.

The surface area and porosity of initial  $\text{NiMoO}_4$  and  $\text{NiMoO}_4$  modified ultrasound for 60 min and 90 min were studied by the isotherm of adsorption / desorption of nitrogen. Type IV hysteresis is observed for three materials (according to IUPAC classification) in the range  $P/P_0$  0.5–1.0 (Fig. 2) and indicates the existence of a mesoporous structure in the materials [12]. The values of the specific surface area determined by the BET (Brunauer–Emmett–Teller) method are presented in Table 1. The specific surface area of the initial nickel molybdate was 31  $\text{m}^2/\text{g}$  and practically does not change for modified materials.

**Table 1**

Structural and adsorption characteristics of the initial  $\text{NiMoO}_4$  and modified by ultrasound for 60 and 90 min.

Sample	$S_{\text{BET}}$ , $\text{m}^2/\text{g}$	$V_{\text{total}}$ , $\text{cm}^3/\text{g}$	d, nm
$\text{NiMoO}_4$	31	0.135	17.4
$\text{NiMoO}_4$ -60	28	0.146	21
$\text{NiMoO}_4$ -90	31	0.223	28.5

The pore size distribution spectra determined by the BJH (Barrett–Joyner–Halenda) method (Fig. 3a) further confirm the mesoporous structure of nickel molybdates and the increase in the average pore size from 17 nm for the initial nickel molybdate to 28.8 nm for ultrasonically modified for 90 min (Table 1). DFT (Density Functional Theory) size distribution histograms indicate a wide pore size distribution in the range of 2 - 26 nm (Fig. 3b, c, d) and an increase in total mesopores volume from 0.135  $\text{cm}^3/\text{g}$  to 0.223  $\text{cm}^3/\text{g}$  with prolonged ultrasonic dispersion.

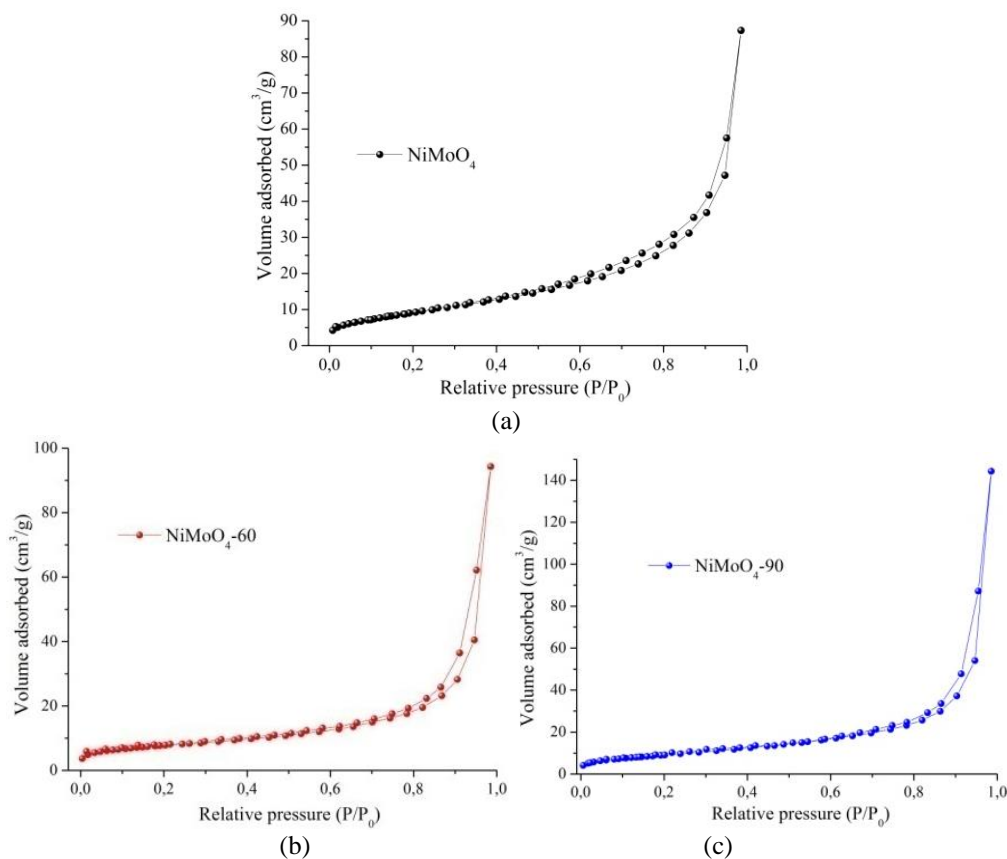


**Fig.2.** Nitrogen adsorption-desorption isotherms ( $-196\text{ }^{\circ}\text{C}$ ) of the (a) initial NiMoO<sub>4</sub> hydrate, NiMoO<sub>4</sub> modified by ultrasound for (b) 60 min and (c) 90 min.

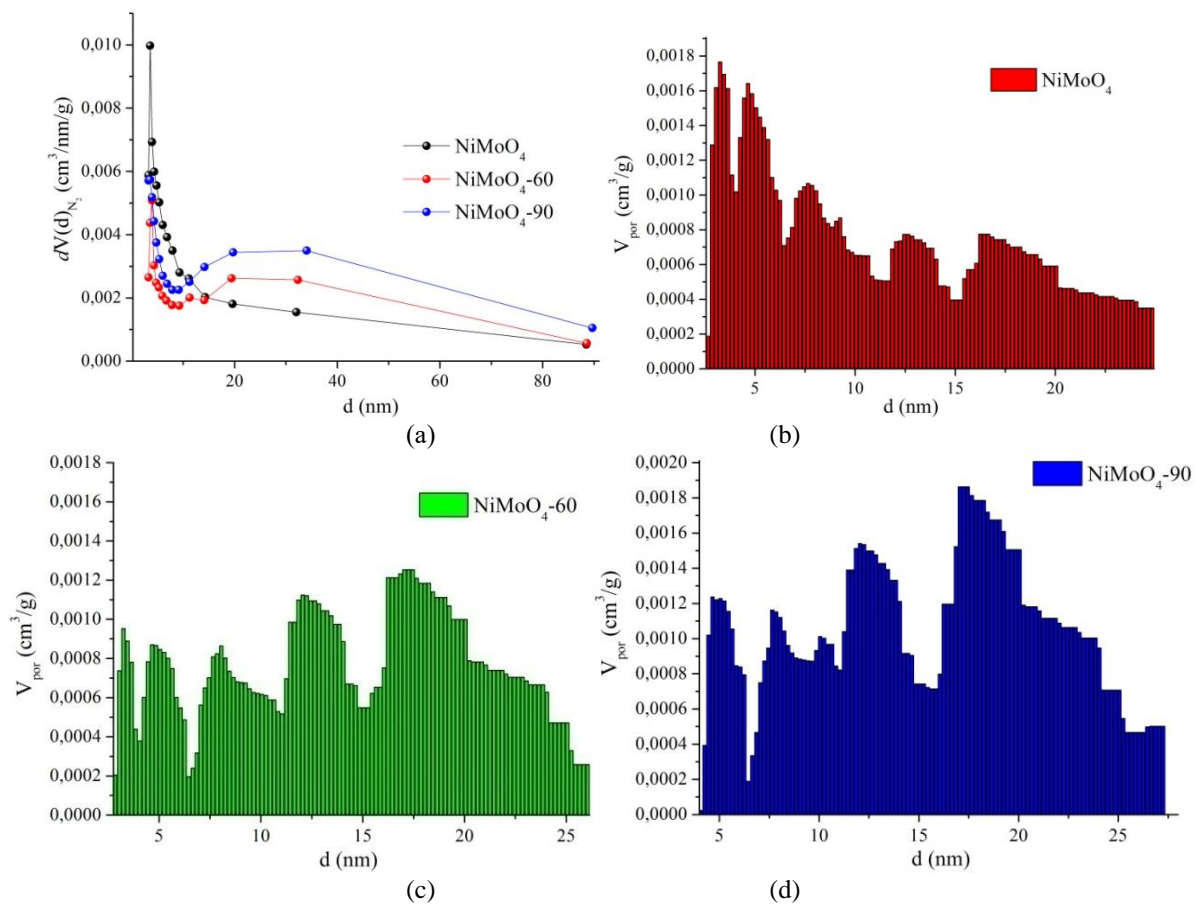


**Fig.3.** (a) BJH pore size distributions plots of the NiMoO<sub>4</sub>, NiMoO<sub>4</sub>-60 and NiMoO<sub>4</sub>-90. DFT pore size distributions plots of the (b) NiMoO<sub>4</sub>, (c) NiMoO<sub>4</sub>-60 and (d) NiMoO<sub>4</sub>-90.

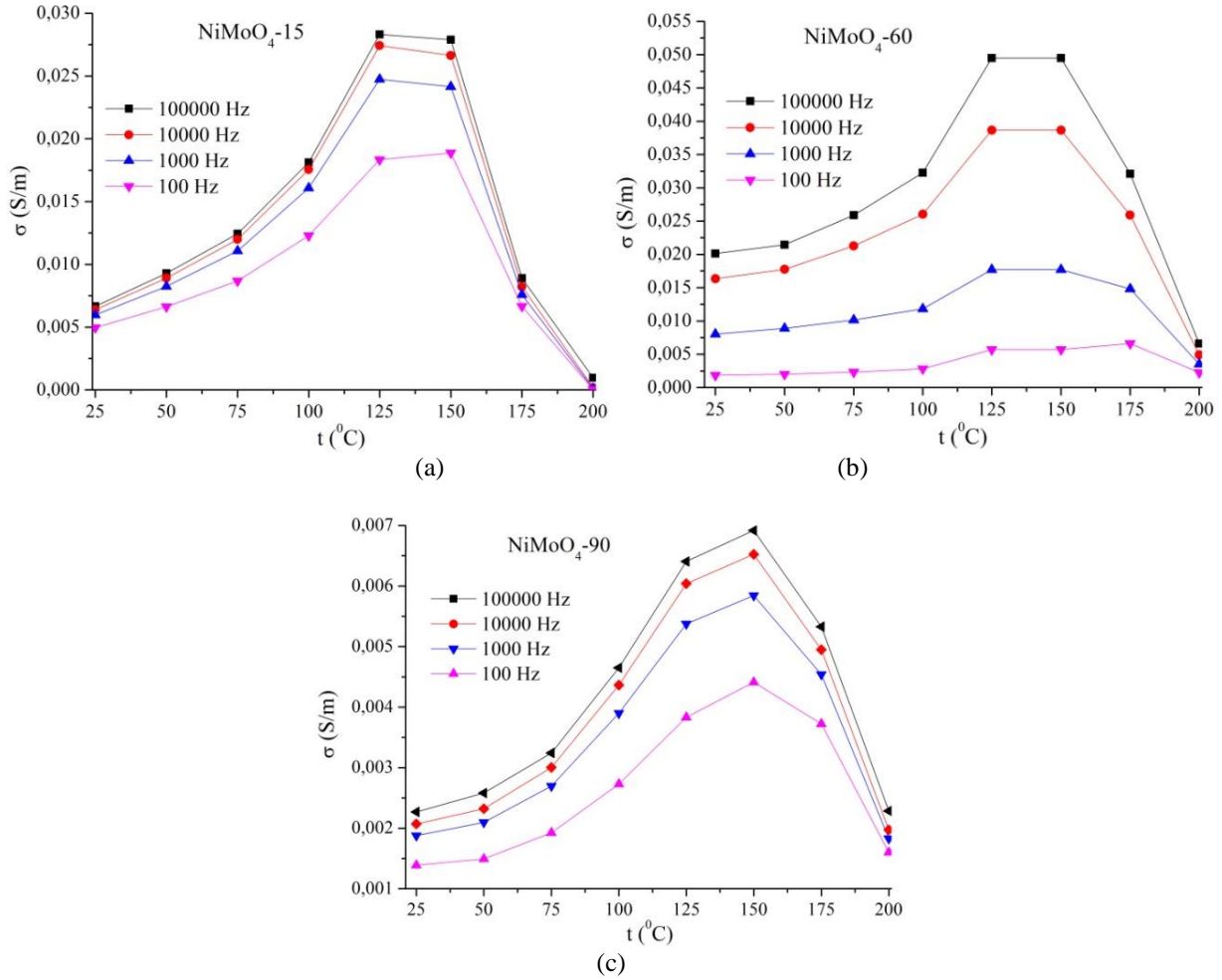


**Fig. 4.** Temperature dependence of AC conductivity of nickel molybdate modified by ultrasound: (a)  $\text{NiMoO}_4\text{-15}$ , (b)  $\text{NiMoO}_4\text{-60}$  and (c)  $\text{NiMoO}_4\text{-90}$ .

Summarizing the data of X-ray analysis and porometry, we conclude that ultrasonic dispersion does not change the size of the crystallites of  $\text{NiMoO}_4$  hydrate, but in modified materials there is a redistribution of pores in size, namely increasing the volume of mesopores with a diameter of 20 - 28 nm. This is due to the fact that at ultrasonic frequencies from 20 kHz to 50 kHz the most common are physical effects, including micro jets and shock waves [13]. For solutions with particles smaller than 0.2 mm, micro jet formation is not possible at frequencies of 22 kHz [7]. Therefore, in such cases, shock waves are created, which accelerate the solid particles suspended in the liquid. Velocities in collisions between particles can reach hundreds of meters per second, causing changes in the morphology of materials [14].

A detailed analysis of the electrical conductivity of the initial hydrate of nickel molybdate is described by us in a previous paper [15]. On the frequency dependences of the conductivity of all samples there is a low-frequency plateau and high-frequency dispersion region, with increasing temperature, the electrical conductivity increases, which is characteristic of semiconductor materials [16]. The temperature dependences of the electrical conductivity of the samples modified by ultrasound at frequencies of  $10^2\text{-}10^5$  Hz are presented in Fig. 4. As for the initial  $\text{NiMoO}_4$  hydrate and for the modified samples there is a decrease in the specific

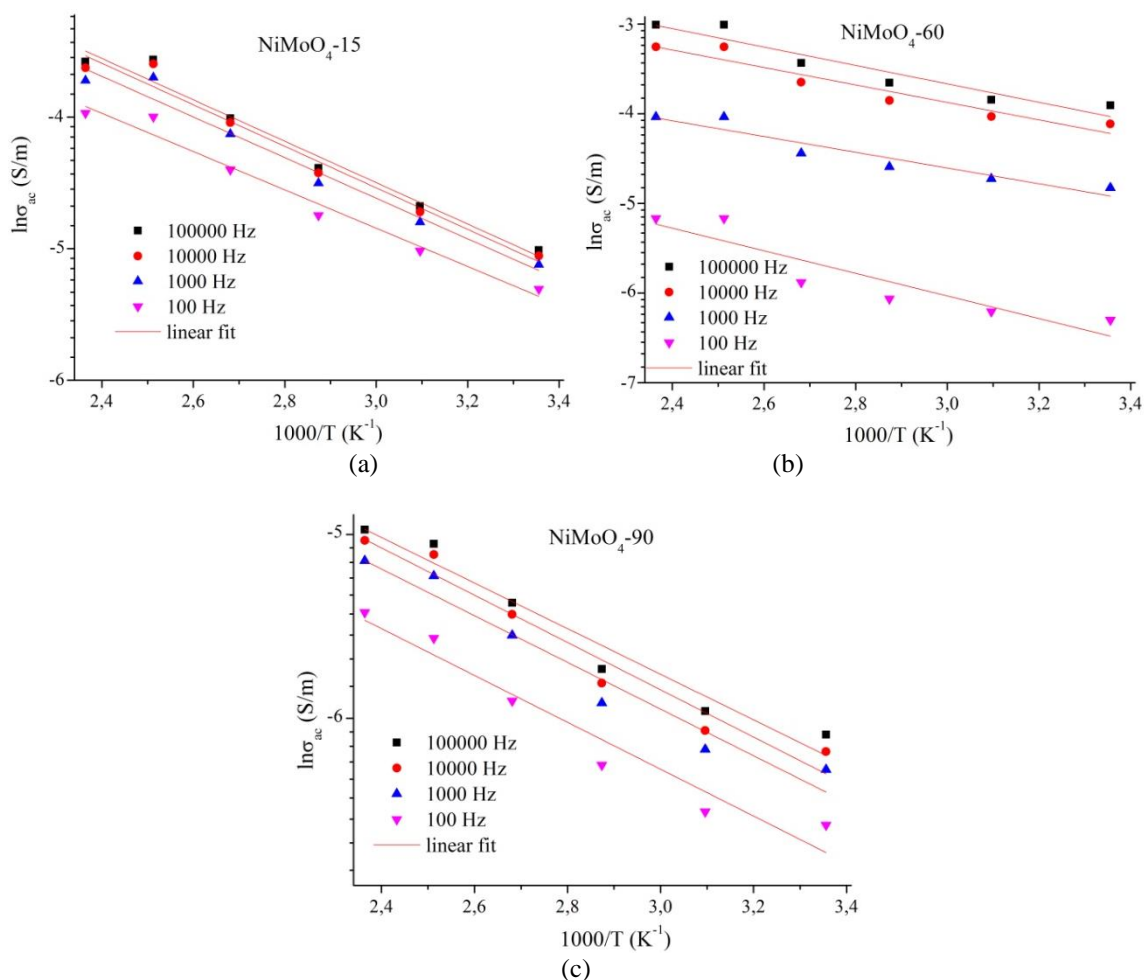
conductivity in the temperature range 175 - 200 °C, which is due to the activation of the mechanism of scattering of charge carriers on the atoms of the crystal lattice. In the high-frequency range ( $10^4 - 10^5$  Hz)  $\text{NiMoO}_4\text{-60}$  has the highest conductivity (Fig.4 b), while at frequencies  $10^2\text{-}10^3$  Hz -  $\text{NiMoO}_4\text{-15}$  has (Fig. 4a).  $\text{NiMoO}_4\text{-90}$  conductivity is the lowest in the entire frequency range (Fig. 4c).

Figure 5 presents the dependence of  $\ln\sigma$  on  $1000/T$ . The activation energy  $E_a$  was calculated from the Arrhenius equation:

$$\sigma = \sigma_0 \exp\left(-\frac{E_a}{k_B T}\right),$$

where  $\sigma_0$  is the pre-exponential coefficient,  $k_B$  is the Boltzmann constant,  $T$  is the absolute temperature, and  $E_a$  is the activation energy. The values of activation energies calculated as a result of  $\ln\sigma$  linearization from  $1000/T$  were 0.12 eV for the initial  $\text{NiMoO}_4$  hydrate [15], 0.13 eV for  $\text{NiMoO}_4\text{-15}$ , 0.09 eV for  $\text{NiMoO}_4\text{-60}$  and 0.11 eV for  $\text{NiMoO}_4\text{-90}$ .

The low activation energy of 0.12 eV for  $\text{NiMoO}_4$  is due to impurities and intrinsic defects present in the materials [15]. The mechanism of surface proton conductivity is possible for modified materials. At 15 min of ultrasonic modification, the activation energy of charge



**Fig. 5.** Arrhenius plots of nickel molybdate modified by ultrasound: (a) NiMoO<sub>4</sub>-15, (b) NiMoO<sub>4</sub>-60 and (c) NiMoO<sub>4</sub>-90.

carriers increases slightly to 0.13 eV, which is due to the transition from surface to bulk conductivity [17], namely, electrical conductivity occurs through hydrogen bonds formed by lattice and coordinated water molecules between NiO<sub>5</sub>(H<sub>2</sub>O) complexes. Subsequent ultrasonic modification leads to changes in the morphology of the surface of nickel molybdate and, accordingly, increase the number of available water molecules and reduce the activation energy. Accordingly, it will increase the number of centers for redox reactions and intercalation / deintercalation of electrolyte ions into the structure of the material, which will positively affect the specific capacitive characteristics of nickel molybdate.

## Conclusions

Based on the results of X-ray analysis and porometry of ultrasonically modified nickel molybdate hydrate, it was found that ultrasound causes mainly physical action on the material by the formation of shock waves. Shock waves lead to redistribution of pores in size, namely the volume of mesopores with a diameter 20 - 28 nm in NiMoO<sub>4</sub>, modified by ultrasound for 60 and 90 min,

increases. At the same time, ultrasonic exposure does not change the crystallite size of the initial and modified materials. In the study of electrical conductivity, it was found that the activation energy of charge carriers of the NiMoO<sub>4</sub>-60 sample is 0.09 eV and is the lowest among the modified materials due to proton conductivity.

## Acknowledgment

*This work was supported by the National Research Foundations of Ukraine [Project No.2020.02/0043].*

**Popovych O.M.** - Doctoral student;  
**Budzulyak I.M.** - Professor, Doctor of Physical and Mathematical Sciences;  
**Kotsyubynsky V.O.** - Professor, Doctor of Physical and Mathematical Sciences;  
**Boyчук V.M.** - Professor, Doctor of Physical and Mathematical Sciences;  
**Illytskyi R.V.** - Professor, Doctor of Physical and Mathematical Sciences;  
**Khemii M.M.** - PhD student;  
**Ivanichok N.Ya.** - Doctoral student;  
**Lezun Ye.V.** - PhD student.

[1] A. González, E. Goikolea, J.A. Barrena & R. Mysyk, Renewable and sustainable energy reviews 58, 1189 (2016); <https://doi.org/10.1016/j.rser.2015.12.249>.

- [2] P.C. Chen, G. Shen, Y. Shi, H. Chen, & C. Zhou, ACS nano 4(8), 4403 (2010); <https://doi.org/10.1021/nm100856y>.
- [3] B.I. Rachiy, B.K. Ostafiychuk, I.M. Budzulyak, V.M. Vashchynsky, R.P. Lisovsky, V. I. Mandzyuk, Journal of Nano-& Electronic Physics 6(4), 04031 (2014); [https://jnep.sumdu.edu.ua/download/numbers/2014/4/articles/jnep\\_2014\\_V6\\_04031.pdf](https://jnep.sumdu.edu.ua/download/numbers/2014/4/articles/jnep_2014_V6_04031.pdf).
- [4] T. Watcharatharapong, M. Minakshi Sundaram, S. Chakraborty, D. Li, G.M. Shafiullah, R.D. Aughterson, & R. Ahuja, ACS Applied Materials & Interfaces 9(21), 17977 (2017); <https://doi.org/10.1021/acsami.7b03836>.
- [5] O. Khemii, I. Budzulyak, L. Yablon, D. Popovych, O. Morushko, R. Lisovskiy, Materials Today: Proceedings 35, 595 (2019); <https://doi.org/10.1016/j.matpr.2019.11.207>.
- [6] V. Boichuk, A. Kachmar, V. Kotsyubynsky, K. Bandura, S. Fedorchenko, Materials Today: Proceedings 50, 423 (2022); <https://doi.org/10.1016/j.matpr.2021.11.243>.
- [7] K.S. Suslick, Science 247(4949), 1439 (1990); <https://doi.org/10.1126/science.247.4949.1439>.
- [8] J.H. Bang & K.S. Suslick, Advanced materials 22(10), 1039 (2010); <https://doi.org/10.1002/adma.200904093>.
- [9] O.M. Popovych, I.M. Budzulyak, V.O. Yukhymchuk, S.I. Budzulyak & D.I. Popovych, Fullerenes, Nanotubes and Carbon Nanostructures 29(12), 1009 (2021); <https://doi.org/10.1080/1536383X.2021.1925253>.
- [10] Y. Ding, Y. Wan, Y.L. Min, W. Zhang, & S.H. Yu, Inorganic Chemistry 47(17), 7813 (2008); <https://doi.org/10.1021/ic8007975>.
- [11] D. Ghosh, S. Giri, & C.K. Das, Nanoscale 5(21), 10428 (2013); <https://doi.org/10.1039/C3NR02444J>.
- [12] G.M. Tomboc & H. Kim, Journal of Materials Science: Materials in Electronics 30(10), 9558 (2019); <https://doi.org/10.1007/s10854-019-01290-4>.
- [13] S.V. Sancheti, P.R. Gogate, Ultrasonics Sonochemistry 36, 527(2016); <https://doi.org/10.1016/j.ultsonch.2016.08.009>.
- [14] H. Xu, B.W. Zeiger, & K.S. Suslick, Chemical Society Reviews 42(7), 2555 (2013); <https://doi.org/10.1039/C2CS35282F>.
- [15] O.M. Popovych, I.M. Budzulyak, O.V. Popovych, V.O. Kotsyubynsky, L.S. Yablon, Journal of Nano-& Electronic Physics 13(6), 06007 (2021); [https://doi.org/10.21272/jnep.13\(6\).06007](https://doi.org/10.21272/jnep.13(6).06007).
- [16] L.O. Shyyko, V.O. Kotsyubynsky, I.M. Budzulyak, P. Sagan, Nanoscale research letters 11(1), 1 (2016); <https://doi.org/10.1186/s11671-016-1451-4>.
- [17] Y.M. Li, M. Hibino, M. Miyayana & T. Kudo, Solid State Ionics 134(3-4), 271 (2000); [https://doi.org/10.1016/S0167-2738\(00\)00759-1](https://doi.org/10.1016/S0167-2738(00)00759-1).

O.M. Попович, I.M. Будзуляк, V.O. Коцюбинський, V.M. Бойчук, P.V. Ільницький,  
M.M. Хемій, H.Я. Іванічок, Є.В. Лезун

## Ультразвукова модифікація нанокристалічного гідрату NiMoO<sub>4</sub>, отриманого гідротермальним методом

Прикарпатський національний університет ім. В. Стефаника, Івано-Франківськ, Україна, [khemiiolha@gmail.com](mailto:khemiiolha@gmail.com)

В роботі представлені результати досліджень кристалічної структури, морфології поверхні та електричних властивостей молібдату нікелю, отриманого гідротермальним методом та модифікованого ультразвуком. Визначено вплив тривалості ультразвукового диспергування на розміри кристалітів, питому площу поверхні, розподіл пор за розмірами та енергію активації носіїв заряду гідрату молібдату нікелю. Встановлено, що ультразвук частотою 22 кГц та тривалістю 90 хв призводить до збільшення загального об'єму мезопор з 0,135 см<sup>3</sup>/г до 0,223 см<sup>3</sup>/г з середнім діаметром 28,5 нм.

**Ключові слова:** молібдат нікелю гідрат, ультразвукова модифікація, питома площа поверхні, електропровідність.